SIMPLIFIED MODEL FOR ANALYSING SOFT IMPACTS ON STRUCTURES: VALIDATION ON STEEL BEAMS

Javier Sánchez-Haro[a], Ignacio Lombillo[b], Guillermo Capellán[c], Begoña Fernández[d], Álvaro Gaute[e].

[a] *Mechanical and Structural Engineering Department of the University of Cantabria, Av. de los Castros 44, Santander 39005, Spain. Researcher, PhD, sanchezja@unican.es*

[b] *Mechanical and Structural Engineering Department of the University of Cantabria, Av. de los Castros 44, Santander 39005, Spain, Professor, PhD, ignacio.lombillo@unican.es*

[c] *Arenas&Asociados Ingeniería de Diseño S.L.P, Marques de la Ensenada 11, 3º, Santander 39009, Spain, CEO, PhD, gcapellan03@gmail.com*

[d] *Arenas&Asociados Ingeniería de Diseño S.L.P, Marques de la Ensenada 11, 3º, Santander 39009, Spain, Estructural Engineer, Msc, bfernandez@arenasing.com*

[e] *Mechanical and Structural Engineering Department of the University of Cantabria, Av. de los Castros 44, Santander 39005, Spain, Professor, PhD, gautea@unican.es*

ABSTRACT

Traditionally, simplified methods have been used to try to solve and understand impacts. These simplified methods sometimes assume hypotheses that excessively limit their applicability or are not sufficiently simplified and require numerical solutions. Thus, to analyse the influence of projectile flexibility in the structural response to impacts, FE models are commonly used due to the limitations of simplified methods. This article proposes a new simplified model that enables the calculation of both structural displacement and contact force during an impact on simple structures, which can be represented as a spring-mass system, such as beams. The model takes into account projectile deformation and the effect of gravitational force on the structural response, providing an analytical solution. The proposed formulation has been validated by means of experimental impact tests and with finite element models of impacts on beams. The effect of gravity, multiple-impacts, and the influence of projectile flexibility when defining soft or hard impact are discussed in depth in this article. This research enables the calculation of complex impacts in an easy way while also facilitating the understanding of the phenomenon and the key parameters for managing it.

KEYWORDS: Soft impact; Projectile flexibility; Structural displacement; Contact force; Gravitational influence; Multiple-Impacts.

HIGHLIGHTS

A general analytical formulation is proposed to solve impacts on structures.

The general analytical formulation solves both displacements and contact forces.

The simplified method considers both projectile and structure flexibility.

The formulation considers the gravitational influence on forces and displacements.

FEM and experimental tests are performed to verify the formulation in 12 cases.

The formulation results match those obtained in the tests and in the FE models.

SYMBOLS

$D_p(t)$	*Projectile displacement at time t*
$D_s(t)$	*Structure displacement at time t*
$d_{s,o}$	*Initial displacement of the structure*
E	*Elastic modulus*
$F(t)$	*Contact force between projectile and structure at time t*
g	*Gravitational acceleration*
H_0	*Height from which the projectile is dropped*
I	*Moment of Inertia*
K_s	*Equivalent stiffness of the structure in the fundamental mode of vibration*
K_p	*Stiffness of the projectile*
L	*Length of the structure*
M_s	*Equivalent mass of the structure in the fundamental mode of vibration*
M_p	*Mass of the projectile*
$M_{p,s}$	*Effective mass of the projectile for the structure during impact*
$M_{p,p}$	*Effective mass of the projectile during the impact*
t_f	*Instant when the impact ends*
t_0	*Instant when the impact begins*

T_p	*Projectile Period of vibration*
T_s	*Structure Period of vibration*
$V_{p,o}$	*Velocity of the projectile the instant just before the impact*
$V_{s,o}$	*Velocity of the structure the instant just before the impact*
$V_p(t)$	*Velocity of the projectile at time t*
$V_s(t)$	*Velocity of the structure at time t*
W_s	*Frequency of vibration in the fundamental mode of the structure*
$W_{s,i}$	*Lowest Frequency of vibration of the structural response during the impact*
W_p	*Frequency of vibration of the projectile*
$W_{p,i}$	*Highest Frequency of vibration of the structural response during the impact*
$W_{s,p}$	*Frequency of vibration of the fundamental mode of the structure modified by the mass of the projectile*
$W_{p,s}$	*Frequency of vibration of the projectile modified by the structure.*
y	*Variable of integration*
α	*Mass ratio between mass of the projectile and equivalent mass of the structure*
α^*	*Mass ratio between equivalent mass of the projectile and equivalent mass of the structure*
ρ	*Density*

1. INTRODUCTION

The potential level of damage that impacts of vehicles, vessels or rockfalls can cause in such slender structures necessitates improvement in knowledge about the behaviour of structures under impact loads [Zhang et al. 2021][Chen et al. 2021][Hao 2015]. The principal design codes treat these impacts as an equivalent static force [Eurocode][AASHTO]. However, it has been demonstrated that this method has obvious drawbacks as it neglects the particular features of dynamic calculations [Zhao et al. 2017][Jin et al. 2020][Zhao and Qian 2019][Gurbuz et al. 2019]. One of the most important parameters when analysing impacts is the deformation of the impacting projectile [Louw et al. 1992]. If the projectile is sufficiently rigid, all the kinetic energy will be transferred to the structure during impact, while if the projectile is deformable, it absorbs deformation energy during the impact which will not be transferred to the structure.

Based on this property, the literature establishes two kinds of impacts, hard impact (rigid projectile) and soft impacts (deformable projectile) [Louw et al. 1992].

The impact process is a complex event but, on many occasions, an accurate simplified method may provide sufficiently accurate results [Abrate 2001]; the key point is knowing when this simplified method can be applied. Simplified methods that consider flexibility of the projectile have been under development for years [Lee et al. 1983][Yang et al. 2012][Yang et al. 2012]. However, even the most recent ones still require relatively complex calculations based on matrix calculations [Lam et al. 2010][Alonso et al. 2019]. In order to assess their accuracy, different simplified methods have been compared [Yang et al. 2012]. It is worth noting that some simplified methods are also being developed but under certain assumptions, such as neglecting the structural mass to avoid considering inertial forces [Al-Thairy and Wang 2013][Utzeri et al. 2021]. However, this hypothesis limits the applicability of the method. Other simplified methods take into account the structural mass but consider only rigid projectiles in calculations [Zhao and Ye 2022]. FE modelling is usually carried out today to solve impacts analysing the influence of projectile deformability in the structural response [Sharma et al. 2012] or even the level of structural damage [Viviani et al. 2021].

This article presents an analytical formulation with two degrees of freedom: a spring-mass system (1DoF) to characterize the projectile, and another spring-mass system (1DoF) to represent simple structures in a simplified form. The theory of impact considering deformable projectiles is based on these mass-spring systems [Chopra 1995]. As a result, the proposed formulation is obtained and verified with transverse impacts on beams through both FE models and experimental tests with well-fitting results. However, beams were chosen to facilitate the experimental campaign in this case. The main novelty of this research is a closed analytical solution to solve impacts. In addition, the frequently neglected effect of acceleration due to gravity is included in the solution. The limits of soft and hard impacts are discussed based on the analytical solution results.

This article is organised as follows: the introduction sets out the general background and the main objectives of the research; in the 'Materials and Methods' section the 12 scenarios (case studies) analysed are presented, explaining the equivalent stiffness and equivalent mass of the structure in each case. Then, detailed descriptions of the FE models are provided, offering enough information to allow any researcher to reproduce the 12 cases studied. The last part of this section describes the measurement system used to obtain the data from the experimental tests. In the next section 'Theory', the projectile's influence is analysed for a general impact considering its deformability, obtaining the proposed formulation used to calculate the impact force and the displacement produced in the structure. In the 'Results and Discussion' section, results are presented and validated by means of FE models and experimental tests, and then they are discussed. The following section 'Additional Checks' analyses the influence of gravity and multiple impacts in order to validate the formulation. Finally, the main conclusions drawn in the investigation are highlighted.

2. MATERIALS AND METHODS

2.1. Case studies

The proposed formulation for simulating elastic impacts has been validated against beams in two ways. On the one hand, displacements have been verified with experimental tests, and on the other hand, contact forces have been checked using FE models (Fig. 1).

With this aim, two beams have been defined. Beam 1 (simple supported steel beam of 1 m long and 0.05x0.01 m^2 cross section, E=2.1·e11 N/m^2, ρ=7,850 Kg/m^3), or a rigid beam, and beam 2 (simple supported steel beam of 1 m long and 0.05x0.004 m^2 cross section, E=2.1·e11 N/m^2, ρ=7,850 Kg/m^3), or a flexible beam.

Different real projectiles with different masses and springs have been used to generate 5 impact cases in both beams, which have been tested in laboratory, as can be seen in Fig. 2.

In [Sánchez-Haro et al. 2022][Sánchez-Haro 2017], some examples of structures transformed into an equivalent 1DoF spring-mass system are provided. For this research, 2 simply supported beams with transverse impacts at the centre have been verified. In [Sánchez-Haro 2017], it is demonstrated that the spring stiffness can be obtained from the expression: $K_s = 48\mathrm{EI}/L^3$ for beams. In the same reference, in an analogous way, it is shown that the effective mass for the same assumption is half of the total mass for beams $M_s = 0.5 \cdot M_{Total}$. The frequency of the fundamental mode of vibration of the spring-mass system, W_s, can be obtained from the expression $W_s = \sqrt{K_s/M_s}$. The mass ratio between projectile and structure defines the parameter $\alpha = M_p/M_s$. In hard impacts, values of this parameter higher than 1 ensure that the fundamental mode of vibration is the main one involved, which means that the impact energy is absorbed mainly by the fundamental mode [Sánchez-Haro et al. 2022]. Thus, values of α higher or slightly lower than 1 have been chosen to analyse the validation of considering only the fundamental mode of vibration in the analysed beams.

Twelve impact cases have been analysed in this article. The total stiffness of the projectile K_p, together with the previously defined parameters for the 12 cases are shown in Table 1. The parameter K_p has been obtained as the sum of the nominal stiffness of each spring. After putting together all the pieces of the projectile, the total stiffness K_p was verified experimentally. Different projectile drop heights H_0 were considered in the impact cases, which define the projectile velocity at the instant just before impact $V_{p,0}$ according to the well-known expression $V_{p,0} = \sqrt{2gH_0}$. The values of $V_{p,0}$ and H_0 for the 12 cases analysed in this article are also shown in Table 1.

The first 5 cases have been defined to check the proposed formulation regarding the displacements of the centre of the beam in experimental tests and FE models. Cases from 5 to 10 have been included specially to verify the contact forces, and they have been modelled only by FE software. Cases 11 and 12 have been added to complete the analysis of hard impact (rigid projectile) vs soft impact (deformable projectile) in this article.

2.2. Description of the models in Midas NFX

The proposed formulation is compared with all the data obtained from the FE software Midas NFX for all the cases [Suthan et al. 2018] [Gridnev and Ravodin 2018]. For each case analysed, the structure was modelled through solid elements, defining a contact without friction between bodies and using a nonlinear explicit transient analysis type. The mesh size of beam 1 is 0.010 x 0.010 x 0.010 while for beam 2, it is 0.010 x 0.010 x 0.004 (length x width x height, in metres). The time increment used for the numerical integration in Midas NFX is 1e.-4 s in all cases. The elastic modulus E_c of the beam has been set to 2.1e8 kN/m^2 and its density to 7850 kg/m^3. In order to reproduce the hypothesis of a deformable projectile, the projectile has been modelled as 2 bodies connected to each other: one to represent the stiffness of the projectile (called *stiffness body*), and the other to represent its mass (*mass body*). The connection between those bodies has been modelled as a series of rigid links, to make sure that both of them move in an analogous manner. In addition, to ensure vertical movement, a series of supports have been added to the sides of both bodies. Both the stiffness and mass bodies are shown in Fig. 3.

The dimensions of the projectiles are compiled in Table 2 for the *mass body* and the *stiffness body*.

The equivalent elastic modulus $E_{c,st}$ of the stiffness body is calculated to reproduce the stiffness of the projectile K_p in each case ($E_{c,st} = \frac{K_p \cdot H_{st}}{W_{st} \cdot L_{st}}$). The body that represents the mass is modelled as a rigid body and, in order to reproduce the hypothesis of an infinitely rigid mass, its elastic modulus $E_{c,m}$ has been set to 1e15 N/m^2.

The self-weight of the springs SW_{sp}in the experimental model is 0.02 kg. To represent that weight in the FE model, a correct density ρ_s is assigned to the *stiffness body* in each case ($\rho_s = \frac{SW_{sp}}{H_s \cdot W_s \cdot L_s}$). Similarly, the density ρ_m of the *mass body* is calculated in each case to represent the mass of the projectile M_p ($\rho_m = \frac{M_p}{H_m \cdot W_m \cdot L_m}$), minus the mass already computed in the *stiffness body*. All cases have been modelled with *stiffness body* 1 except cases 3 and 8 that have been modelled with *stiffness body* 2 in order to avoid errors due to numerical convergence. The values of these parameters for FEM analysis are shown in Table 3.

To model the impact with the software Midas NFX, the same nodal force was set at the nodes of each element of the projectile in order to simulate the acceleration due to gravity. These nodal forces (Table 3) have been applied to the projectile (54 nodes) in each case. All cases were calculated with the explicit method of Midas NFX, Fig. 4.

Vertical displacement results have been obtained directly from the software. However, contact forces come from the solid stresses in the vertical direction in all nodes of a section of the *stiffness body*. The stresses of each node have been multiplied by the corresponding influence area. A summation of all of them has been made to obtain the total contact force.

2.3. Description of the measurement system in experimental tests.

To empirically characterize the structural response of the beams, the authors have installed one unit of Tokyo Sokki FCA-3-11-1L bidirectional strain gauge to determine the deformation undergone [Dally et al. 1978][Iriarte et al. 2021] by the lower fibre of the beams on their mid-span section. The bidirectional strain gauge band is made up of two bands, the first is oriented in the direction of the strain that is intended to be experimentally determined and the second is oriented in the direction perpendicular to this strain. Both bands are connected to each other by means of an electronic mounting in a half Wheatstone bridge that enables compensation for thermal phenomena during the course of the test [Iriarte et al. 2021][Hoffmann 2012]. The acquisition, recording and monitoring of the information provided by the sensors is carried out through a Structural Monitoring System (SMS) composed of the following elements: a) a NI-CDAQ-9188 modular central data acquisition and processing unit (MCDA&PU), with the capacity to simultaneously manage the signal from up to eight Data Acquisition Units (DAU); (b) a NI-9237 extensometer that powers the Wheatstone Bridge's electronic assembly of the extensometers and the treatment of the analogue signal from these sensors [Dally et al. 1978][Iriarte et al. 2021][Hoffmann 2012]; (c) a workstation responsible for communicating with the MCDA&PU and recording and viewing data provided by sensors through a Data Acquisition and Monitoring Program designed and programmed by the authors (Fig. 5).

Due to the dynamic features of the test, the measurement was done with a calibrated extensometer because of the absence of friction that it introduces into the system.

3. THEORY

3.1. Initial Hypothesis

Initially, some assumptions must be defined in order to state and solve the problem of impact of a deformable projectile on structures. The closer the initial assumptions are to the actual impact conditions, the closer the results of the formulation are to the exact ones. The following is a description of the assumptions adopted.

Hypothesis 1: The structure is composed of an isotropic linear elastic material, indicating that the stiffness properties remain constant throughout the entire impact. If this assumption is not satisfied, a reasonable approximation of the impact can be achieved with the proposed formulation by using the average stiffness over the impact duration, e.g., in an inelastic impact.

If the material is not isotropic, the stiffness properties have to be calculated considering this effect in the direction of the structural response.

Hypothesis 2: The structure is initially at rest, i.e., it has no movement.

Hypothesis 3: Regarding impacts where bending is the primary resistance mechanism, shear and axial forces, as well as local deformation, have not been considered in the simplified model (however, they have obviously been accounted for in the FE models and experimental tests conducted). Thus, in bending impacts axial forces (or membrane forces in 2D structures) could only exert influence with significant displacements, but such effects are not anticipated under the test conditions or in the structures analyzed. Nevertheless, the influence of axial or membrane forces can be incorporated into the proposed simplified method by accounting for their impact on the parameter *Ks*. Shear forces and local deformation increase the total displacement, so they have some influence depending on the case. However, the aim of the paper is to analyse the impact easily in order to predesign structures and to check FEM results. Thus, it does not make sense to include them in the formulation if the contribution is limited and they do not modify the general behaviour of structures under impact loads. Local and shear deformation are not important from a predesign or verification point of view. In any case, the correctness of these hypotheses will be analysed later.

Hypothesis 4: The projectile is considered deformable in comparison to the stiffness of the structure.

Hypothesis 5: The projectile has no dimensions, it is assumed to act at a point.

Hypothesis 6: The initial velocity of the projectile is perpendicular to the structure. Furthermore, the impact is considered elastic, that is, viscous behaviour from the materials is excluded.

Hypothesis 7: Structural damping has not been considered due to the short duration of the impact, which does not allow for significant energy dissipation. The proposed formulation analyzes the time taken to reach the first peak of displacement, where the maximum contact force has already occurred, thus this initial peak is not significant affected by the normal damping ratios. Additionally, energy losses due to heat or noise during the impact are not accounted for the same reason.

Hypothesis 8: The impact is centred, that is, the point of contact and the centres of gravity are aligned.

Hypothesis 9: The impact begins when the projectile contacts the structure ($\mathrm{t_0}$), and ends when the contact force becomes a tension ($\mathrm{t_f}$). This contact is considered continuous from $\mathrm{t_0}$ to $\mathrm{t_f}$.

3.2. Problem description

A projectile mass M_p and a projectile stiffness K_p is assumed with velocity $V_p(t)$ in a perpendicular direction to the structure. The fundamental mode of the structure has an effective mass M_s and an effective stiffness K_s, initially being at rest ($t < t_0$), Fig. 6(a). When the impact between the structure and the projectile begins ($t = t_0$), the projectile has an initial impact velocity $V_{p,0}$, the structure remains at rest, and the contact force between the bodies $F(t)$ has not developed yet, and hence its value is null, Fig. 6(b). From this point on ($t > t_0$), because of the impact, the structure deforms at the same time as the projectile's velocity reduces. At any moment between the beginning and the end of the impact ($t_0 < t < t_f$), the displacement of the projectile $D_p(t)$ and the structure $D_s(t)$ are the same because of the initial hypotheses, Fig 6(c).

Equations (1) and (2) express, respectively, these displacements at time t. Note that dissipative forces, represented as a viscous damper in Fig. 6 (constant C is the viscous damping coefficient), are neglected due to the fact that the impact occurs so fast that structural damping has no time to develop significantly. Moreover, note that is not necessary to consider acceleration due to gravity in the mass of the structure since the structure is balanced prior to impact. Thus, the gravitational acceleration g only influences the projectile during the impact.

It has been demonstrated that a spring-mass system can represent the dynamic behaviour of a vehicle during a collision [Al-Thairy and Wang 2014], so this kind of projectile considered as a spring-mass system has a wide-ranging applicability in real cases if the final solution of the simplified method is correct.

Based on the previous problem description, the displacement of the projectile (1) and the displacement of the structure (2) can be defined in the following equations:

$$D_p(t) = V_{p,0} \cdot t - \iint_0^t \frac{F(t)}{M_p} dt\, dt - \frac{F(t)}{K_p} + \iint_0^t g\, dtdt + d_{s,o} \tag{1}$$

$$D_s(t) = V_{s,0} \cdot t + \iint_0^t \frac{F(t) - K_s(D_s(t))}{M_s}\, dt\, dt \tag{2}$$

By developing the following change of variable expressed in equation (3), equation (1) and (2) can be expressed as equations (4) and (5).

$$\frac{d^4 y}{dt^4} = \ddddot{y} = F(t) \tag{3}$$

$$D_p(t) = V_{p,o} \cdot t - \frac{\ddot{y}}{M_p} - \frac{\ddddot{y}}{K_p} + \frac{1}{2} g t^2 + d_{s,o} \tag{4}$$

$$D_s(t) = \frac{K_s + K_p}{M_s K_p}\ddot{y} + \frac{K_s}{M_s M_p} y + -\frac{K_s\, g}{24 M_s} t^4 - \frac{K_s V_{p,o}}{6 M_s}\, t^3 - \frac{d_{s,o} K_s}{2 M_s} t^2 + V_{s,0} \cdot t + d_{s,o} \tag{5}$$

While contact between structure and projectile happens $D_p(t) = D_s(t)$, and rearranging in equations (4) and (5), equation (6) is obtained

$$M_{p,p}((V_{p,o} - (V_{s,o})t + \frac{d_{s,o} w_s^2 + g}{2} t^2 + \frac{w_s^2 V_{p,o}}{6}\, t^3 + \frac{w_s^2\, g}{24} t^4) = w_{s,p}^2 y + \ddot{y} + \frac{\ddddot{y}}{w_{p,s}^2} \tag{6}$$

Note that natural vibration frequency of the structure W_s and the natural vibration frequency of the projectile W_p before impact can be obtained from expressions (7) and (8), respectively.

$$W_s = \sqrt{\frac{K_s}{M_s}} \tag{7}$$

$$W_p = \sqrt{\frac{K_p}{M_p}} \tag{8}$$

In equation (6) there are some parameters requiring clarification. Firstly, the frequency of the structure modified by the projectile $w_{s,p}$ (equation (9)) and the frequency of the projectile modified by the structure $w_{p,s}$ (equation (10)), assuming both vibrate without interfering with each other's vibration, are defined below.

$$w_{s,p} = \sqrt{\frac{K_s}{M_s + M_{p,s}}} \tag{9}$$

$$w_{p,s} = \sqrt{\frac{K_p}{M_{p,p}}} \tag{10}$$

Where the effective mass of the projectile considered in the frequency of the structure $M_{p,s}$ and the effective mass of the projectile considered in the frequency of the projectile $M_{p,p}$ are defined in equations (11) and (12).

$$M_{p,s} = M_p\left(1 + \frac{K_s}{K_p}\right) \tag{11}$$

$$M_{p,p} = M_p\left(\frac{1}{1 + \frac{M_p}{M_s}\left(1 + \frac{K_s}{K_p}\right)}\right) = M_p\left(\frac{1}{1 + \frac{M_{p,s}}{M_s}}\right) \tag{12}$$

It is worth highlighting that $\frac{M_{p,s}}{M_p} \geq 1$ and $\frac{M_{p,p}}{M_p} \leq 1$. This means that during the impact the structure considers an effective mass of projectile heavier than the real mass in the modification of its natural frequency (equation (9)), and the projectile considers a lighter mass of itself in its own vibration (equation (10)).

3.2.1. Problem resolution

The general solution y of equation (6) can be found as the sum of the particular solution y_P and the homogeneous solution y_H (equation (13)).

$$
\begin{gathered}
y = y_P + y_H \\
y_P = P_1 t^4 + P_2 t^3 + P_3 t^2 + P_4 t + P_5 \\
y_H = H_1 \, sin(W_{p,i}\, t) + H_2 \, cos(W_{p,i}\, t) + H_3 \, sin(W_{s,i}\, t) + H_4 \, cos(W_{s,i}\, t)
\end{gathered}
\tag{13}
$$

Coefficients of the particular solution y_P from P_1 to P_5 can be obtained if the particular solution is substituted into equation (6), simply by matching "t" terms with the same power. The coefficients found for the particular solution are shown in equation (14).

$$
\begin{gathered}
P_1 = \frac{M_p}{24} g \; ; \; P_2 = \frac{V_{p,o} M_p}{6} ; \;\; P_3 = \frac{(M_{p,p} - M_p) g + M_{p,p} d_{s,o} {W_s}^2)}{2{W_{s,p}}^2} \\
P_4 = \frac{V_{p,o}\left(M_{p,p} - M_p\right) - V_{s,o} M_{p,p}}{{W_{s,p}}^2} \; ; \; P_5 = -\frac{M_p g}{{W_{s,p}}^2 {W_{p,s}}^2} - \frac{(M_{p,p} - M_p) g + M_{p,p} d_{s,o} {W_s}^2}{{W_{s,p}}^4}
\end{gathered}
\tag{14}
$$

The coefficients of the homogenous solution y_H (H_1 to H_4) in equation (13) can be obtained by simply applying the following initial conditions. The first initial condition results from making the impact force null at $t = 0$, $F(t_0) = \frac{d^4 y}{dt^4} = 0$ (equation (3)). The second initial condition results from attributing an initial displacement $d_p(t = 0) = d_{s,o}$ (equation (4)). The third initial condition results from attributing an initial velocity of the projectile $V_p(t = 0) = \frac{d(d_{p\,(t=0)})}{\mathrm{dt}} = V_{p,0}$ (derivative of equation (4)).The fourth initial condition results from attributing an initial velocity of the structure $V_s(t = 0) = \frac{d(d_{s\,(t=0)})}{\mathrm{dt}} = V_{s,0}$ (derivative of equation (5)). Note that $V_{s,0}$ will be zero at the first impact because the structure is at rest, but in a case with multiple impacts, it will not be zero in the additional impacts.

The coefficients of the homogenous solution (H_1 to H_4) after applying the above initial conditions are shown in equation (15).

$$
\begin{gathered}
H_1 = \frac{M_p V_{p,o} - H_3 {W_{s,i}}^3}{{W_{p,i}}^3} \; ; \qquad H_3 = \frac{-\frac{M_p V_{p,o}}{{W_{p,i}}^2} - \frac{V_{p,o}\left(M_{p,p} - M_p\right) - V_{s,o} M_{p,p}}{{W_{s,p}}^2}}{\frac{{W_s^*}^3}{{W_{p,i}}^2} - W_s^*} \\
H_2 = -H_4 \frac{{W_s^*}^4}{{W_p^*}^4} - \frac{g M_p}{{W_p^*}^4} ; \qquad H_4 = \frac{\frac{g M_p}{{W_{p,i}}^2} + \frac{(M_{p,p} - M_p) g + M_{p,p} d_{s,o} {W_s}^2}{{w_{s,p}}^2}}{{W_{s,i}}^2 - \frac{{W_{s,i}}^4}{{W_{p,i}}^2}}
\end{gathered}
\tag{15}
$$

Equation (13) shows the two frequencies of the structural response. The higher frequency $W_{p,i}$ is related to the frequency of the projectile during impact and the lower frequency $W_{s,i}$ is related to the frequency of the structure during impact. Both are defined in equation (16).

$$W_{p,i} = \sqrt{\frac{1}{2}{W_{p,s}}^2 (1 + \sqrt{1 - 4(\frac{W_{sp}}{W_{ps}})^2})} \; ; \; W_{s,i} = \sqrt{\frac{1}{2}{W_{p,s}}^2 (1 - \sqrt{1 - 4(\frac{W_{sp}}{W_{ps}})^2})} \tag{16}$$

Thus, substituting the appropriate derivative of equation (13) into equations (3) and (5), the analytical closed-form expression for structural displacements (17) and contact forces (18) in impacts can be expressed as follows:

$$\begin{aligned} D_s(t) = {} & d_{s,o} + V_{p,o} \cdot t + \frac{1}{2} g t^2 - \frac{M_p g}{K_p} + (\frac{{W_{p,i}}^2}{M_p} - \frac{{W_{p,i}}^4}{K_p})\, H_1 sin(W_{p,i}\, t) + (\frac{{W_{p,i}}^2}{M_p} \\ & - \frac{{W_{p,i}}^4}{K_p}) H_2 cos(W_{p,i}\, t) + (\frac{{W_{s,i}}^2}{M_p} - \frac{{W_{s,i}}^4}{K_p}) H_3 sin(W_{s,i}\, t) + (\frac{{W_{s,i}}^2}{M_p} \\ & - \frac{{W_{s,i}}^4}{K_p}) H_4 cos(W_{s,i}\, t) - \frac{12 P_1 t^2 + 6 P_2 t + 2 P_3}{M_p} \end{aligned} \tag{17}$$

$$\begin{aligned} F(t) = {} & {W_{p,i}}^4 H_1\, sin(W_{p,i}\, t) + {W_{p,i}}^4 H_2 cos(W_{p,i}\, t) + {W_{s,i}}^4\, H_3 sin(W_{s,i}\, t) + {W_{s,i}}^4\, H_4\, cos(W_{s,i}\, t) \\ & + M_p g \end{aligned} \tag{18}$$

In order to study the multiple impacts before the projectile is totally stopped, the research considers when the contact between structure and projectile does not happen. The criteria to define when this contact takes place is defined in equation (19).

$$F(t) \geq 0 \tag{19}$$

The structure and the projectile will be separated at instant *t'* when the condition expressed in equation (19) is not met due to the fact that contact forces cannot develop tension forces. In that situation, both the structure and projectile will have independent movements. The structure will move under free vibrations, equation (20), and the projectile under uniform acceleration, equation (21).

$$d_s(t) = d_s(t') \cos(w_s(t - t')) - \frac{V_s(t')}{w_s} \sin(w_s(t - t')) \tag{20}$$

$$d_p(t) = d_s(t') + V_p(t')(t - t') - \frac{1}{2} g (t - t'\,)^2 \tag{21}$$

While there is no contact, $d_s(t) > d_p(t)$. Contact will take place again at instant t'' when the displacement of the projectile and the displacement of the structure will be the same. Thus the criterion for the new contact is expressed in equation (22).

$$d_p(t'') = d_s(t'') \tag{22}$$

From the instant t'', and while equation (22) is fulfilled again, equations (4) and (5) can be applied to produce the new impact, considering the time variable to be t-t'' and the initial velocities and displacements of the structure and projectile just before this new impact, equation (23).

$$d_{s,o} = d_s(t''); \; V_{s,o} = V_s(t''); \; V_{p,o} = V_p(t'') \tag{23}$$

All the following impacts can be analysed in the same way as was explained previously.

Finally, the equivalent mass of the projectile from the structure's point of view defines a new ratio of masses α^* for soft impacts.

$$\alpha^* = \frac{M_{p,s}}{M_s} \tag{24}$$

The last consideration in the theoretical basis of the previous *Deformable Projectile* theory and, consequently, the proposed formulation, is that the parameters of the structure defining the fundamental mode K_s have been considered to be elastic for the sake of simplicity of the laboratory test. If the secant line in the stress-strain curve of the material and inertia modifications are considered in parameter K_s, the inelastic behaviour of the structure can also be modelled with the proposed formulation in an iterative process. Additionally, parameter K_s can be incremented to take into account, for example, membrane forces or another type of hardening. Thus, considering that different types of structures can be modelled and considering the proposed formulation can be adapted to assess anything from membrane forces to inelastic behaviour of structures in an easy way, the simplified method is widely applicable. The aim of this article is to establish the basis of the simplified method, so general elastic cases have been verified, but more complex cases will be analysed in further research.

4. RESULTS AND DISCUSSION

4.1. Displacements Results

The first step in the validation of the proposed formulation defined in the previous section is to check the solution for the displacement at the centre of the beam under impact. To do so, the displacements in cases 1 to 5 are compared with experimental tests and FE model results. Thus, from the impact parameters (equivalent stiffness, equivalent masses, etc.) previously calculated, Table 1, and through equation (17), the theoretical results obtained using the simplified model considering a *Deformable Projectile* are shown in Fig. 7, comparing them with those of the FE models and the experimental tests. Additionally, the impact solution for a *Rigid Projectile* defined in [Sánchez-Haro et al. 2022] is included in order to have a reference as if the impact was hard. It is worth highlighting that case 1 and case 2 are similar, excepting the beam under impact. In case 1 the structure under impact is beam 2 (the flexible one) and in case 2 the beam 1 (the rigid one). Therefore, the mass of the projectile, the stiffness of the projectile and projectile drop heights are exactly the same. However, the response of the beam in case 1 (Fig. 7(a)) is closer to hard impact behaviour and in case 2 (Fig. 7(b)) it is clearly different, that is, a soft impact.

The structural response of the beam for the Deformable Projectile defined in section 3 is based on two waves. The wave related to the frequency $W_{p,i}$ depends mainly on the projectile, while the frequency $W_{s,i}$ depends mainly on the structure. In the five cases shown in Fig. 7, the main wave is associated with $W_{s,i}$ and the wave which oscillates on the main wave is associated with $W_{p,i}$. The mechanical system of springs in the projectile for the experimental tests has a big damping effect (more than 15%) while the steel beam has a small damping effect (around 1%). For this reason in the experimental tests the wave associated with $W_{s,i}$ can be seen fully developed but the wave associated with $W_{p,i}$ undergoes greater difficulties to fully develop. In any case, the results obtained by means of the proposed formulation considering a *Deformable Projectile*, FE models and experimental tests clearly fit well. Maximum displacements of the structure, $D_s(t)$, from cases 1 to 5 are summarized in Table 4 to check the relative error between the simplified model considering a *Deformable Projectile*, the FE models and test results.

As can be seen in Table 4, the relative error regarding the maximum displacement between the simplified model results and the FE model results is less than of 8%. Additionally, both curves fit quite well during the whole impact test in all cases shown in Fig. 7. Case 2 has a null relative error because both curves are perfectly matched. The relative error between the simplified method results and the experimental test results are slightly larger but less than 11% in all cases shown in Table 4. The large damping of the spring's mechanism is the cause of this difference, as was commented before. In any case, the shape of the displacement versus time curves is well matched in all cases depicted in Fig. 7. Fig. 7(f) shows a comparison of cases 1, 3 and 5 in order to demonstrate how the simplified method adapts to different scales and shapes.

4.2. Force results

The second step in the validation of the proposed formulation defined in section 3 is to check the solution for the contact force between the structure and the projectile, equation (18). It is important to emphasize that the validation of the contact force is significantly more accurate than the validation of the displacement. This is because the contact force is the fourth derivative of the solution function (equation (3)), whereas the displacement is derived as the second derivative (equation (5)). In this regard, the contact force and also the displacements of cases 6 to 10 are compared with the FE model results in Fig. 8.

As can be seen in Fig. 8, the displacement and force results match very well. Maximum displacements of the structure, $D_s(t)$, and contact forces from cases 6 to 10 are summarized in Table 5 to check the relative error between the simplified model considering a *Deformable*

Projectile and the FE models, both in terms of displacements and forces. Note that the relative error shown in Table 5 in contact forces is slightly higher than in displacements.

As can be seen in Table 5, the relative error regarding the maximum displacement between the simplified model and the FE model results is less than 4%. In addition, both curves are quite well matched during the whole impact test in all the cases depicted in Fig. 8. Regarding the contact force, the relative error between the simplified method and the FE model results is slightly larger but less than 7% in all cases shown in Table 4. This increase in error is due to the presence of higher modes of vibration which are negligible regarding displacements. These higher modes of vibration can be neglected as long as parameter $\alpha^* > 1$ [Sánchez-Haro et al. 2022]. In any case, the shapes of the contact force versus time curves match well in all the cases, as shown in Fig. 8. Fig. 8(f) shows a comparison of cases 7, 9 and 10 in order to demonstrate how the simplified method adapts to different scales and shapes also for force results.

4.3. Soft impact Vs. Hard Impact.

Usually, the limit between a rigid impact and a soft impact is established based on the parameter T_p/T_s. If $\frac{T_p}{T_s} > 1$, it is considered a deformable impact, while if $\frac{T_p}{T_s} \ll 1$, it is considered as a rigid impact [Al-Thairy and Wang 2014]. Table 6 shows this ratio for the 12 cases studied in this article.

Case 1 (beam 2) and case 2 (beam 1), both with the same projectile and the projectile drop heights, present $\frac{T_p}{T_s}$ values of 0.61 and 1.52, respectively. Based on the observations from Fig. 7(a) and Fig. 7(b), it would seem that the classical definition works perfectly.

As this research obtained a closed formulation for impacts, where the stiffness of the projectile is a parameter, and it is easy to increase the number of cases analyzed, case 11 and case 12 were added.

Firstly, deformable impact according to its classical definition has been analysed. Case 3, case 6 and case 11 have values of $\frac{T_p}{T_s} \gg 1$, so deformable impacts would be expected. In order to compare these cases in the same graph, non-dimensional axes of displacement and time have been used in Fig. 9. The displacement of the projectile has been divided by the maximum displacement obtained as a *Rigid Projectile*, while the time has been divided by the time it takes for the structure to return to its pre-impact equilibrium position if the impact were rigid. This enables a graphical comparison of how close cases 3, 6, and 11 are to rigid impact.

Cases 3 and 6 clearly exhibit deformable impacts because their curves differ significantly to *Rigid Projectile* curves. However, case 11 shows a curve similar to a *Rigid Projectile* curve. The key is in the parameter $W_{p,i}/W_{s,i}$ (Table 6), which compares how the number of waves associated with $W_{p,i}$ fits with a wave associated with $W_{s,i}$. As shown in Fig. 9, the curve in case 3 ($W_{p,i}/W_{s,i} = 3.72$) and the curve in case 6 ($W_{p,i}/W_{s,i} = 3.11$) have comparable wave amplitudes. In case 11 ($W_{p,i}/W_{s,i} = 9.27$), the amplitude of the curve associated with $W_{p,i}$ is much smaller than that of the wave associated with $W_{s,i}$, and the oscillation of the wave $W_{p,i}$ around the main wave $W_{s,i}$ is easily noticeable. Based on this analysis, it can be concluded that the parameter $\frac{T_p}{T_s} > 1$ alone is not sufficient to define a soft impact, and the parameter $W_{p,i}/W_{s,i}$ needs to be considered.

Secondly, impacts with parameter $\frac{T_p}{T_s} < 1$ have been analysed. Thus, for cases 1 and 12, rigid impacts would be expected under the classical definition. As shown in Fig. 10, the curve in case 1 $\left(\frac{T_p}{T_s} = 0.61\right)$ is very similar to the curve of a *Rigid Projectile*, but the curve in case 12 $\left(\frac{T_p}{T_s} = 0.73\right)$ shows a very different shape to the *Rigid Projectile* one. In this analysis, the parameter $W_{p,i}/W_{s,i}$ is also key. Case 1 has a ratio of $W_{p,i}/W_{s,i} = 9.76$, while case 12 has a ratio of $W_{p,i}/W_{s,i} = 3.09$. Therefore, based on the previous analysis, it can be concluded that the parameter $\frac{T_p}{T_s} < 1$ is not sufficient to define a rigid impact, and the parameter $W_{p,i}/W_{s,i}$ needs to be considered.

In the same way as the classical definition, the proposed limit between hard and soft behaviour is qualitative. It is not easy to define an exact limit to know whether an impact should be classified as hard or soft because it is a progressive process. However, based on the analysis of the 12 cases described in this article and their results, the following recommendation is proposed:

- If $\frac{T_p}{T_s} > 2.5$, the impact should always be considered as soft.
- If $\frac{T_p}{T_s} < 2.5$ and the parameter $W_{p,i}/W_{s,i} < 5$, the impact should be considered as soft.
- If $\frac{T_p}{T_s} < 2.5$ and the parameter $W_{p,i}/W_{s,i} > 5$, the impact can be considered as hard.

The recommendation has been formulated to clarify when the rigid projectile formulation or the flexible projectile formulation can be applied. There are other parameters that may influence the separation between hard and soft impacts, such as projectile velocity and local penetration. However, these parameters are of lesser importance compared to the proposed parameters, and for the sake of simplicity , they have not been considered.

4.4. Limitation of the proposed formulation

The simplified method shown in [Sánchez-Haro et al. 2022] to solve impacts under the hypothesis of a rigid projectile demonstrates that the ratio between the projectile mass and the equivalent mass of the structure (α parameter) defines whether the fundamental mode is enough to represent the dynamic behaviour of simple structures. In this regard, the main conclusion in that reference was that if $\alpha > 1$ then the fundamental mode absorbs the majority of the energy of the impact. Thus if $\alpha < 1$ more than one mode of vibration would be needed to represent the dynamic behaviour of the structure. In Table 1, the values of the α parameter in the 12 cases analysed in this paper are presented. As can be seen in Fig. 7(d), case 4 ($\alpha = 0.95$) does not exhibit any significant contribution of higher modes of vibration in either FEM or experimental results.

For a deformable projectile, the effective mass of the projectile from a structural point of view is defined in equation (11). Similarly to the α parameter for a Rigid Projectile, shown in [Sánchez-Haro et al. 2022], the Deformable Projectile requires that the parameter α^*, defined in equation (24), takes values greater than 1 to ensure that there is no large influence of higher modes of vibration. Table 6 presents the values of the parameter α^* in the 12 cases analysed in this investigation, and as can be observed in all cases, $\alpha^* > 1$. This is the reason why there is no significant vibration due to higher modes of vibration.

5. ADDITIONAL CHECKS

5.1. Influence of Gravity.

There is a lack of knowledge in the literature about the influence of gravity on impacts, as can be seen in the main reference books [Goldsmith 2001][Stronge 2004]. Only in the case of hard impacts, has gravity been considered recently [Sánchez-Haro et al. 2023]. In order to verify whether the proposed formulation considers the effect of gravity correctly, case 3 has been analysed using a value of $g=9.806 m/s^2$, Fig. 11(a), and also using a value of $g=0\ m/s^2$, Fig. 11(b).

As can be seen in Fig. 11, the proposed formulation considers the effect of gravity in an appropriate way as the FE model and Experimental curves are much better matched with the simplified model considering a *Deformable Projectile* curve in Fig. 11(a) than in Fig. 11(b).

5.2. Multiple impacts

In this section, the suitability of the proposed formulation for reproducing all the multiple impacts that take place during the whole impact is verified. To this end, a specific analysis of case 1 has been performed.

Firstly, case 1 has been calculated without considering the condition defined in equation (19) and compared with FE model. This means that the contact force could develop tension forces in the proposed formulation. As can be verified in Fig. 12(a), tension forces exist for the first time around 0.02s. Fig. 12(b) illustrates that the displacement curves are in complete agreement before 0.02s, but diverge after that point.

Case 1 has been recalculated considering the condition defined in equation (19). Note that the contact force shown in Fig. 13(a) is always greater than zero. In this second analysis, the displacement curves between the FE model and the the simplified model considering a *Deformable Projectile* fit much better, as can be verified in Fig. 13(b). As a result, it can be observed that case 1 undergoes 5 impacts before the beam returns to its equilibrium position. Based on this analysis, it can be concluded that the proposed formulation is capable of accurately reproducing the multiple impacts that occur during a collision.

6. CONCLUSIONS

The research presented is an adaptation of the rigid impact theory referenced throughout this article, aimed primarily at incorporating the effect of projectile flexibility (i.e., considering the projectile's deformation energy during impact), as well as the effects of gravity and multiple impacts. Because the original rigid impact theory was applicable to various types of simple structures, the soft impact theory developed here also maintains that general applicability to different simple structural systems, as the initial methodology has been preserved. Therefore, this new formulation has been validated only on beams, which have been transformed into spring-mass systems for the application of the proposed formulation. In this article, twelve cases of soft impacts were analysed in two different beams and in all of them the suggested simplified model considering a deformable projectile provided results well-fitted to those offered by FE models and experimental tests, both for displacements and contact forces. The proposed formulation matched the peak of forces, the maximum displacements, and the modification of frequency of vibration of the structure during the impact, and in general both the displacement time-history and acceleration time-history were well matched. The structural damping was not considered in the proposed formulation since, for typical values, the dissipation occurring in the first wave produced after each impact is very small. The matched results obtained have shown that this simplification is acceptable for the purposes of the proposed formulation. The investigation also shows that some considerations such as shear strain and local deformations are not necessary to approximate the general behaviour of the structure under impact load. Other effects not considered in this article, such as axial stiffening, can be easily incorporated into the formulation by adding the axial stiffness term to the general stiffness.

Regarding the gravity influence and multiple impacts, specific checks were performed to prove the accuracy of the proposed formulation and good results were obtained.

In order to easily identify when the rigid impact formulation or the soft impact formulation is applicable, the classic limit ($\frac{T_p}{T_s} = 1$) was analyzed in the article. Some cases were found in which this parameter does not represent the limit in an accurate way. An additional parameter $W_{p,i}/W_{s,i}$ was proposed to complement the classical criteria. New limits for both classical and new parameters are proposed. Other parameters for the differentiation between rigid and soft impact have not been considered because the ones analyzed are sufficient for a qualitative separation that indicates which formulation is applicable.

Similarly to what happens with rigid impact theory and the parameter α, a limitation in the proposed formulation based on the parameter α^* was established. Values of $\alpha^* > 1$ mean that the fundamental mode of vibration is sufficient when reproducing the dynamic behaviour of a structure under impact loads, because that mode of vibration absorbs the majority of the impact energy. Regarding the main advantages of the proposed formulation, it can be summarized in three points. Firstly, the proposed formulation enables structural engineers to perform checks on FE model results easily, in the same way that engineers do in static cases. Secondly, a fundamental aspect enabled by the formulation is the integration of impact analysis into the design phase and alternative studies. The time required to calculate impacts in complex models under impact loads is substantial, often deferred until the final solution is reached. Having an agile tool for decision-making will allow for more efficient structural design against impact loads. Finally, the proposed formulation is also useful to establish the integration parameters in a FEM model, greatly reducing the computational cost, because impact duration, maximum displacement and maximum contact force are already well known from the proposed formulation.

This article has fundamentally established the basis of the proposed formulation. However, further research in ongoing to show that this formulation can be applied in more complex structures such as plates, bridges, etc. and will be addressed in future research, as well as the inelastic behaviour of structures.

7. ACKNOWLEDGEMENT

We would like to thank *Simulsoft Ingenieros España* for lending the Midas NFX software for use in this research, which has been of great help.

8. DATA AVAILABILITY STATEMENT

Some or all data, models, or code that support the findings of this study are available from the corresponding author upon reasonable request.

9. REFERENCES

AASHTO LRFD Bridge Design Specifications.

Abrate, S. 2001. "Modeling of impacts on composite structures". *Composite Structures*, vol.51, no 2, pp. 129-138. https://doi.org/10.1016/S0263-8223(00)00138-0.

Alonso, J., J. A. Parra, A. Pacios, and M. C. Huerta. 2019. "Similarity index: A procedure for comparing impact time histories validated with soft impact test". *Engineering Structures*, vol. 198. https://doi.org/10.1016/j.engstruct.2019.109513.

Al-Thairy, H., and Y. C.Wang. 2013. "A simplified analytical method for predicting the critical velocity of transverse rigid body impact on steel columns". *International Journal of Impact Engineering*, vol. 58 pp. 39-54. https://doi.org/10.1016/j.ijimpeng.2013.02.004.

Al-Thairy, H., and Y. C. Wang. 2014. "Simplified FE vehicle model for assessing the vulnerability of axially compressed steel columns against vehicle frontal impact". *Journal of Constructuctional Steel Research*, vol. 102, pp. 190-203. https://doi.org/10.1016/j.jcsr.2014.07.005.

Chen, L., H. Wu, and T. Liu. 2021. "Vehicle collision with bridge piers: A state-of-the-art review". *Advances in Structural Engineering*, vol. 24, no. 2, pp. 385-400. https://doi.org/10.1177/1369433220953510.

Chopra, A. K.. 1995. "Dynamics of Structures. Part 1". Book, Prentice-Hall.

Dally, J. W., and W. F. Riley. 1978. "Experimental stress analysis". Book, McGraw Hill. https://doi.org/10.1016/0142-1123(81)90011-6.

Eurocode 1- BS EN 1991-1-7: - Accidental actions.

Gridnev, S., and I. Ravodin. 2018. "Finite element modeling of a moving load using contact conditions". *Theorical Foundation of Civil Engineering*, vol. 196. https://doi.org/10.1051/matecconf/201819601044.

Goldsmith, W.. 2001. "Impact". Book, Courier Corporation.

Gurbuz, T., A. Ilki, D. P. Thambiratnam, and N. Perera. 2019. "Low-Elevation Impact Tests of Axially Loaded Reinforced Concrete Columns". *ACI Structural Journal*, vol 116, no 1, pp.117-128. https://doi.org/10.14359/51710862.

Hao, H.. 2015. "Predictions of structural response to dynamic loads of different loading rates". *International Journal of Protective Structures*, vol. 6, no. 4, pp 585-605. https://espace.curtin.edu.au/handle/20.500.11937/6075.

Hoffmann, K.. 2012. "An introduction to stress analysis and transducer design using strain gauges". Book, HBM.

Iriarte, X., J. Aginaga, G. Gainza, J. Ros, and J. Bacaicoa. 2021. "Optimal strain-gauge placement for mechanical load estimation in circular cross-section shafts". *Measurement*, vol. 174. https://doi.org/10.1016/J.MEASUREMENT.2020.108938.

Jin, L., Y. Lan, R. Zhang, and X. Du. 2020. "Impact resistance of RC beams under different combinations of mass and velocity: mesoscale numerical analysis". *Archives of Civil and Mechanical Engineering*, vol. 20, no. 4. https://doi.org/10.1007/S43452-020-00129-8.

Lam, N. T. K., H. H. Tsang, and E. F. Gad. 2010. "Simulations of response to low velocity impact by spreadsheet". *International Journal of Structructural Stability and Dynamics*, vol. 10, no. 3, pp. 483-499. https://doi.org/10.1142/S0219455410003580.

Lee, Y., J. F. Hamilton, and J. W. Sullivan. 1983. "The Lumped Parameter Method for Elastic Impact Problems". *Journal of Applied Mechanics*, vol. 50, no. 4a, pp. 823–827. https://doi.org/10.1115/1.3167152.

Louw, J. M., G. Maritz, and M. J. Loedolff. 1992. "The behaviour of RC columns under impact loading". *Journal of Civil Engineering*, vol. 34, no 11. https://hdl.handle.net/10520/EJC25142.

Sánchez-Haro, J.. 2017. "Development of theory on impacts: simplified method of calculation of impacts in structures". Dr. Thesis, University of Cantabria. https://repositorio.unican.es/xmlui/handle/10902/11461.

Sánchez-Haro, J., I. Lombillo, and G. Capellán. 2022. "Equivalent Static Force in Heavy Mass Impacts on Structures". *International Journal of Structructural Stability and Dynamics*, vol. 22, no. 02. https://doi.org/10.1142/S0219455422500250.

Sánchez-Haro, J., I. Lombillo, and G. Capellán. 2023. "Simplified model to consider influence of gravity on impacts on structures: Experimental and numerical validation". *International Journal of Impact Engineering*. vol. 173, 104474. https://doi.org/10.1016/j.ijimpeng.2022.104474.

Sharma, H., S. Hurlebaus, and P. Gardoni. 2012. "Performance-based response evaluation of reinforced concrete columns subject to vehicle impact". *International Journal of Impact Engineering*, vol. 43, pp. 52-62. https://doi.org/10.1016/j.ijimpeng.2011.11.007.

Stronge, W. J.. 2004. "Impact Mechanics". Book, Cambridge University.

Suthan, R., V. Jayakumar, and S. Madhu. 2018. "Evaluation of Mechanical Properties of Kevlar Fibre Epoxy Composites: An Experimental Study". *International Journal of Vehicle Structures and Systems*, vol. 10, no. 6, pp. 389-394. https://doi.org/10.4273/ijvss.10.6.02.

Utzeri, M., M. Sasso, G. Chiappini, and S. Lenci. 2021. "Modelling of Low-velocity Impacts on Composite Beams in Large Displacement". *Fracture and Structural Integrity*, vol. 15, no. 58, pp. 254-271. https://doi.org/10.3221/IGF-ESIS.58.19.

Viviani, L., A. Consolaro, M. Maffeis, and G. Royer-Carfagni. 2021. "Engineered modelling of the soft-body impact test on glazed surfaces". *Engineering Strucuctures*, vol. 226. https://doi.org/10.1016/j.engstruct.2020.111315.

Yang, Y., N. T. K. Lam, and L. Zhang. 2012. "Evaluation of simplified methods of estimating beam responses to impact". *International Journal of Structructural Stability and Dynamics*, vol. 12, no. 3. https://doi.org/10.1142/S0219455412500162.

Yang, Y., N. T. K. Lam, and L. Zhang. 2012. "Estimation of response of plate structure subject to low veloctiy impact by a solid object". *International Journal of Structructural Stability and Dynamics*, vol. 12, no. 6. https://doi.org/10.1142/S0219455412500538.

Zhang, C., G. Gholipour, and A. A. Mousavi. 2021. "State-of-the-Art Review on Responses of RC Structures Subjected to Lateral Impact Loads". *Archives of Compututational Methods Engineering*, vol. 28, no. 4, pp. 2477-2507. https://doi.org/10.1007/S11831-020-09467-5.

Zhao, D., W. Yi, and S. K. Kunnath. 2017. "Shear Mechanisms in Reinforced Concrete Beams under Impact Loading". *Journal of Structural Engineering*, vol. 143, no 9. https://doi.org/10.1061/(ASCE)ST.1943-541X.0001818.

Zhao, W., and J. Qian. 2019. "Dynamic Response and Shear Demand of Reinforced Concrete Beams Subjected to Impact Loading". *International Journal of Structructural Stability and Dynamics*, vol. 19, no. 8. https://doi.org/10.1142/S0219455419500913.

Zhao, W., and J. Ye. 2022. "Dynamic behavior and damage assessment of RC columns subjected to lateral soft impact". *Engineering Structures*, vol. 251. https://doi.org/10.1016/j.engstruct.2021.113476.

10. TABLES

Case	**Beam**	M_S **(kg)**	**K$_s$ (N/m)**	W_s **(Rad/s)**	M_p **(kg)**	K_p **(N/m)**	**α** (M_p/M_s)	H_0 **(m)**	**V$_{p,0}$ (m/s)**
1	2	0.78	2,688	58.52	3.63	33.68	4.62	0.10	1.40
2	1	1.96	42,000	146.29	3.63	33.68	1.85	0.10	1.40
3	1	1.96	42,000	146.29	3.63	8.32	1.85	0.05	0.99
4	1	1.96	42,000	146.29	1.87	8.32	0.95	0.10	1.40
5	1	1.96	42,000	146.29	5.40	33.68	2.76	0.10	1.40
6	1	1.96	42,000	146.29	3.63	18.92	1.85	0.10	1.40
7	1	1.96	42,000	146.29	5.40	33.68	2.76	0.03	0.78
8	2	0.78	2,688	58.52	3.63	8.32	4.65	0.01	0.44
9	2	0.78	2,688	58.52	1.87	8.32	2.40	0.10	1.40
10	2	0.78	2,688	58.52	1.87	4.56	2.40	0.01	0.44
11	2	0.78	2,688	58.52	10.89	9.12	13.87	0.05	0.99
12	1	1.96	42,000	146.29	1.87	75.68	0.95	0.10	1.40

Table 1. Definition of structural parameters of the projectiles and impact parameters in each case.

Mass body	**Length, L$_m$ (m)**	**Width, W$_m$ (m)**	**Height, H$_m$ (m)**
	0.02	0.05	0.02
Stiffness body	**Length, L$_{st}$ (m)**	**Width, W$_{st}$ (m)**	**Height, H$_{st}$ (m)**
1	0.02	0.05	0.05
2	0.02	0.05	0.10

Table 2. FE model definition: *mass body* and *stiffness body* of the projectile.

Case	ρ_m **(kg/m^3)**	ρ_s**(kg/m^3)**	$E_{c,s}$**(N/m^2)**	$F_{node}(N)$
1	181500	400	1684	0.659
2	181500	400	1684	0.659
3	181500	200	832	0.659
4	93500	400	416	0.340
5	270000	400	1684	0.981
6	181500	400	946	0.659
7	270000	400	1684	0.981
8	181500	200	832	0.659

9	93500	400	416	0.340
10	93500	400	228	0.340
11	544500	400	456	1.978
12	93500	400	3784	0.340

Table 3. Values of parameters for FEM analysis.

Case	Simplified model -deformable projectile- (m)	FE models (m)	Relative error[(1)] (%)	Experimental tests (m)	Relative error[(2)] (%)
1	$6.31 \cdot 10^{-2}$	$6.16 \cdot 10^{-2}$	2.4	$5.69 \cdot 10^{-2}$	10.9
2	$1.30 \cdot 10^{-2}$	$1.30 \cdot 10^{-2}$	0.0	$1.17 \cdot 10^{-2}$	11.0
3	$5.62 \cdot 10^{-3}$	$5.85 \cdot 10^{-3}$	3.9	$5.21 \cdot 10^{-3}$	7.8
4	$6.38 \cdot 10^{-3}$	$6.93 \cdot 10^{-3}$	7.9	$5.95 \cdot 10^{-3}$	7.2
5	$1.49 \cdot 10^{-2}$	$1.50 \cdot 10^{-2}$	0.6	$1.36 \cdot 10^{-2}$	8.9

[(1)] Displacement relative error (Simplified model considering Deformable Projectile – FE models)
[(2)] Displacement relative error (Simplified model considering Deformable Projectile – Experimental tests)

Table 4. Maximum displacement (m) and relative error (%) for cases 1 to 5.

Case	Maximum displacement			Maximum force		
	Simplified model -deformable project.- (m)	FE models (m)	Relative error[(1)] (%)	Simplified model -deformable project.- (kN)	FE models (kN)	Relative error[(2)] (%)
6	$1.12 \cdot 10^{-2}$	$1.16 \cdot 10^{-2}$	3.3	$3.09 \cdot 10^{-1}$	$3.25 \cdot 10^{-1}$	4.9
7	$8.63 \cdot 10^{-3}$	$8.60 \cdot 10^{-3}$	0.4	$3.27 \cdot 10^{-1}$	$3.33 \cdot 10^{-1}$	1.8
8	$3.40 \cdot 10^{-2}$	$3.42 \cdot 10^{-2}$	0.7	$1.04 \cdot 10^{-1}$	$1.04 \cdot 10^{-1}$	0.4
9	$3.88 \cdot 10^{-2}$	$3.85 \cdot 10^{-2}$	0.8	$1.56 \cdot 10^{-1}$	$1.64 \cdot 10^{-1}$	4.8
10	$1.88 \cdot 10^{-2}$	$1.85 \cdot 10^{-2}$	1.7	$5.73 \cdot 10^{-2}$	$6.16 \cdot 10^{-2}$	7.0

[(1)] Displacement relative error (Deformable projectile – FE model)
[(2)] Force relative error (Deformable projectile – Experimental model)

Table 5. Maximum displacement (m), force (kN) and relative error (%) for cases 6 to 10.

Case	T_p	T_s	T_p/T_s	$W_{p,i}$	$W_{s,i}$	$W_{p,i}/W_{s,i}$	α*	Rigid (R) / Deformable (D)
1	0.07	0.11	0.61	234.59	24.04	9.76	4.99	R
2	0.07	0.04	1.52	207.97	67.76	3.07	4.16	D
3	0.13	0.04	3.05	161.43	43.43	3.72	11.17	D
4	0.09	0.04	2.19	162.82	60.03	2.71	5.75	D
5	0.08	0.04	1.85	203.96	56.65	3.60	6.18	D

6	0.09	0.04	2.03	181.27	58.26	3.11	5.96	D
7	0.08	0.04	1.85	203.94	56.65	3.60	6.18	D
8	0.13	0.11	1.22	125.88	22.28	5.65	6.12	R
9	0.09	0.11	0.88	132.83	29.45	4.51	3.15	D
10	0.13	0.11	1.18	104.52	27.70	3.77	3.78	D
11	0.22	0.11	2.02	125.38	13.52	9.27	17.96	R
12	0.03	0.04	0.73	301.59	97.65	3.09	1.48	D

Table 6. Periods and frequencies for 12 cases analysed.

11. LIST OF FIGURES

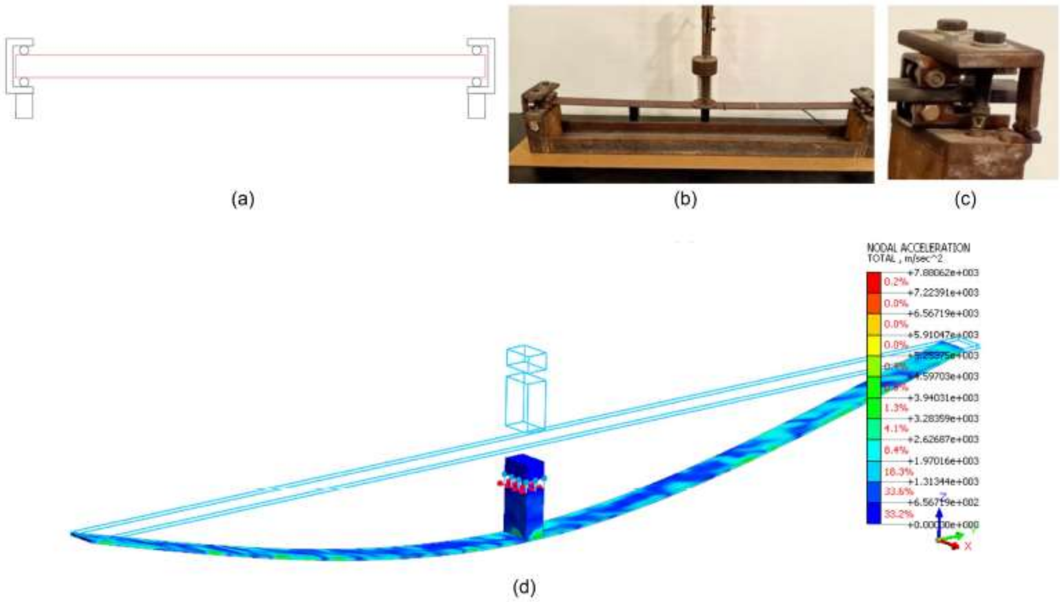

Fig. 1. Structures studied: (a) sketch of beams; (b) beam 1 test; (c) simple support; and (d) beam FE model.

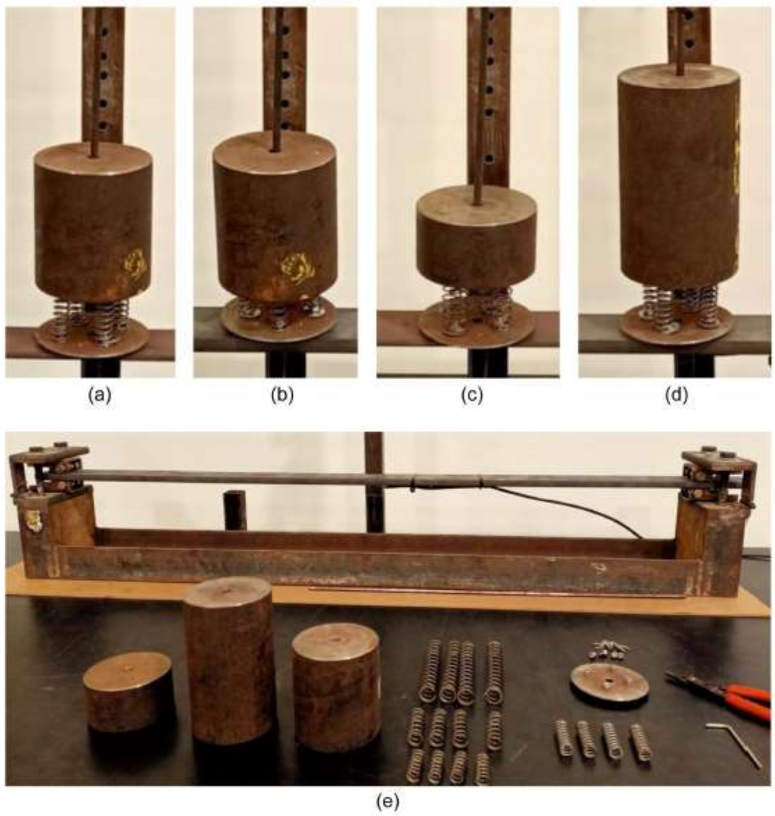

Fig. 2. Deformable projectile (steel): (a) projectile in Cases 1 and 2; (b) projectile in Case 3; (c) projectile in Case 4; (d) projectile in Case 5; and (e) set of 3 masses and 4 kinds of springs used in the whole research.

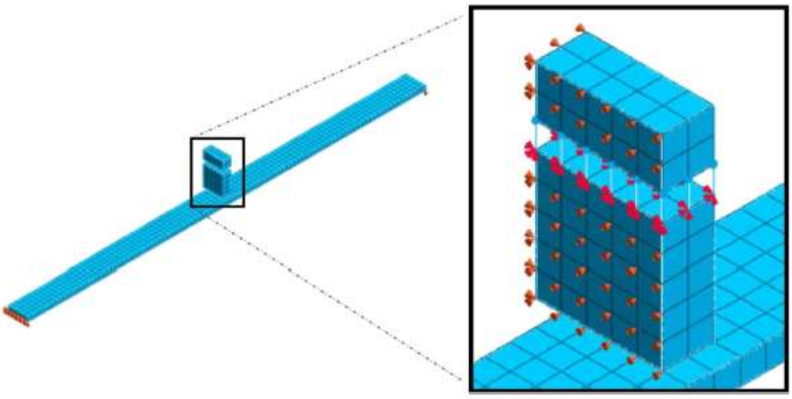

Fig. 3. FE model: connection between stiffness body (lower) and mass body (upper) and lateral supports added to ensure vertical movement.

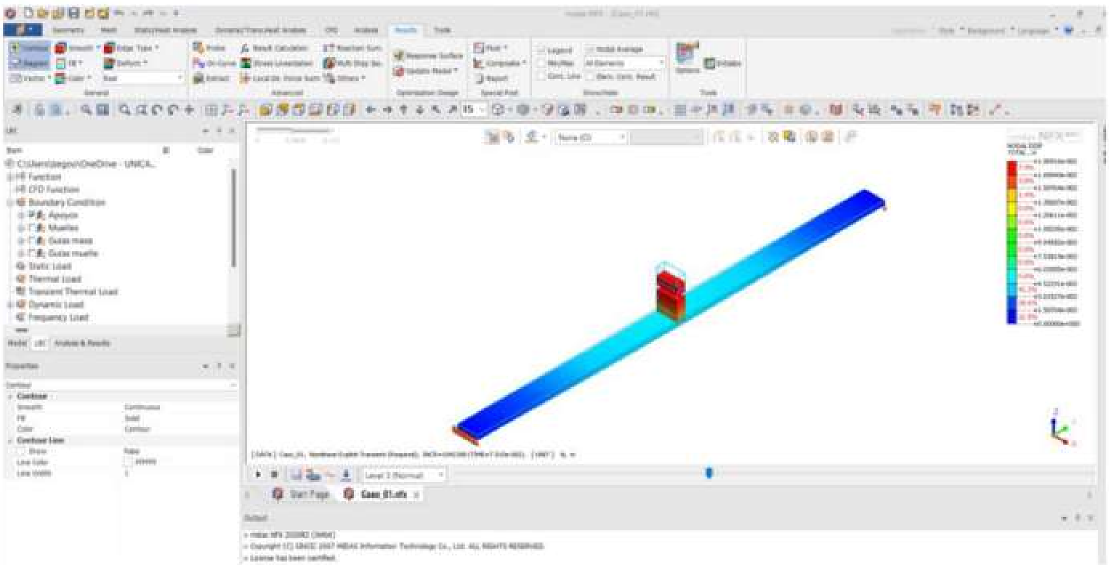

Fig. 4. FE model: impact output data analysis.

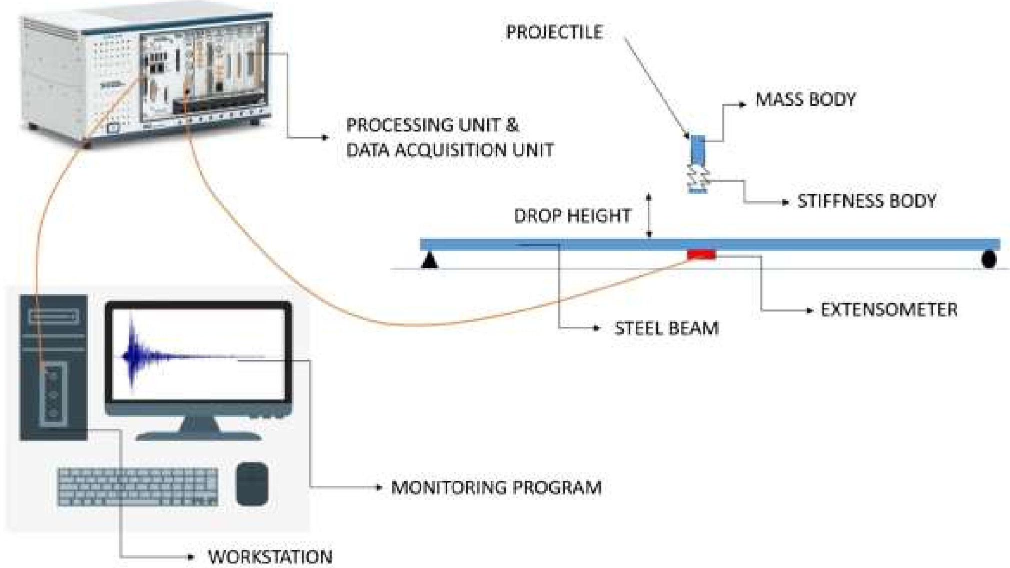

Fig. 5. Real-time display of the deformation undergone by the lower fibre of the beam span centre.

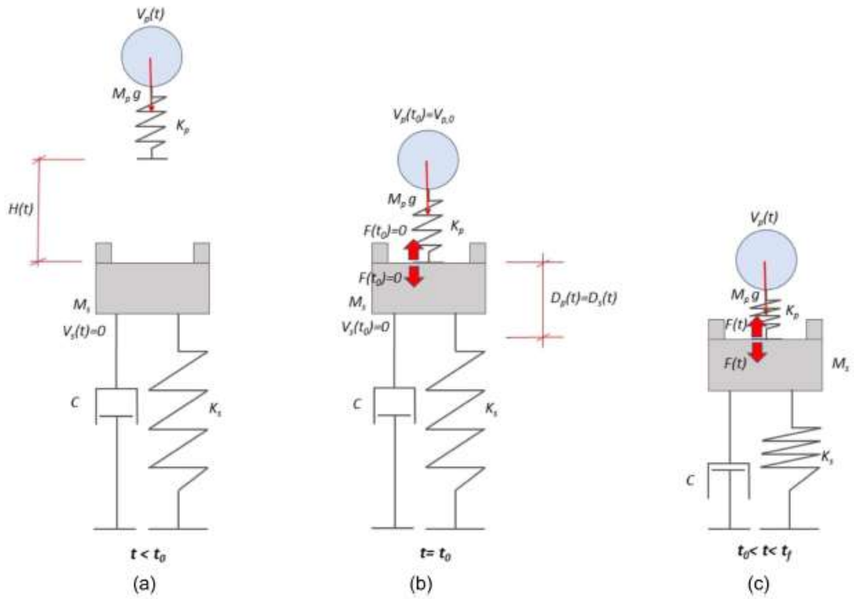

Fig. 6. Idealized impact sequence: (a) situation before the impact between the structure and the projectile; (b) instant of impact ($t = t_0$); and (c) situation between the beginning and the end of the impact ($t_0 < t < t_f$). (Data from Sánchez-Haro et al. 2022.)

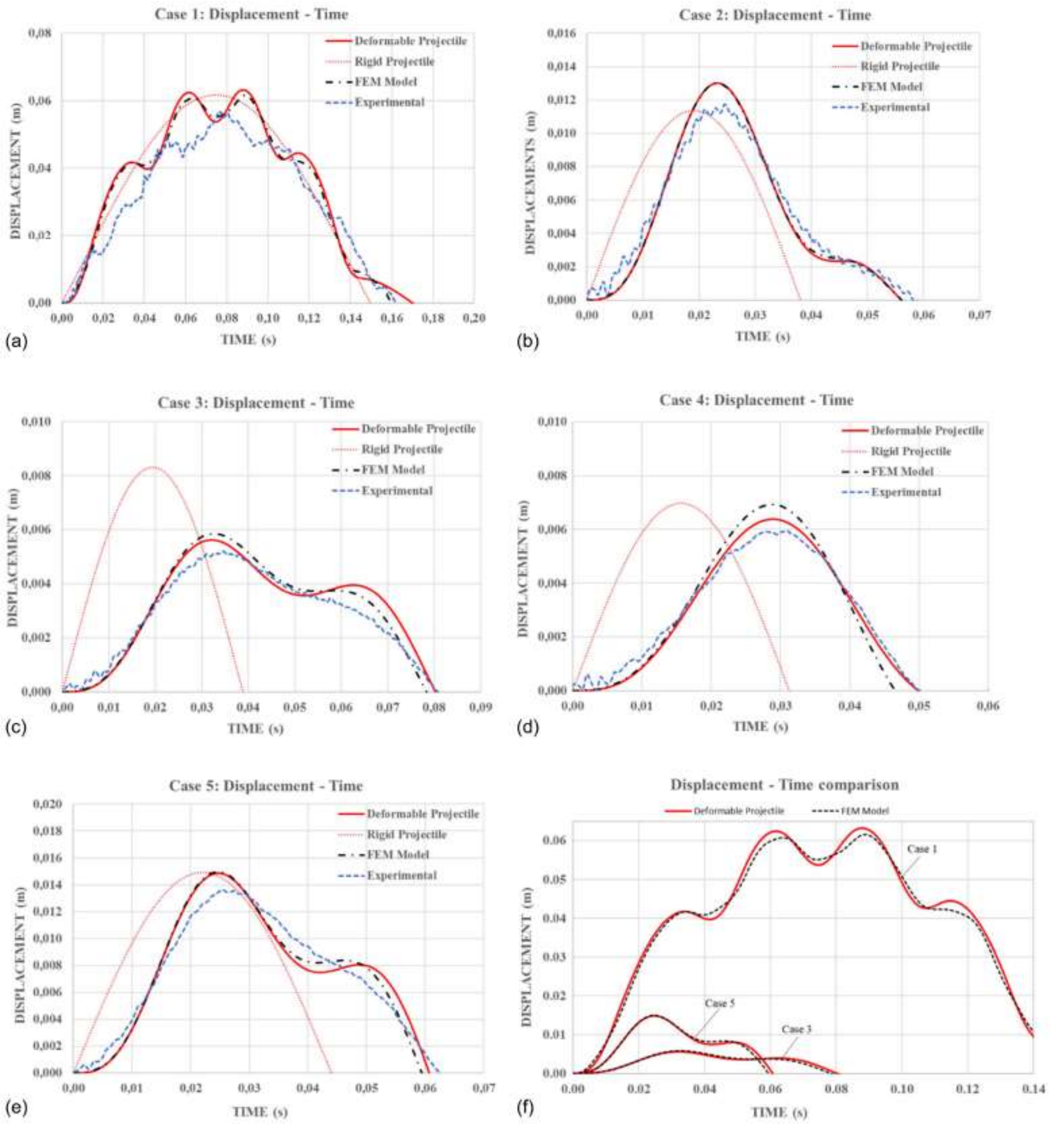

Fig. 7. Comparison between the results obtained using the simplified model considering a *Deformable Projectile*, the FE models, and the tests: (a) Case 1; (b) Case 2; (c) Case 3; (d) Case 4; (e) Case 5; and (f) Case 1, Case 3, and Case 5 comparison.

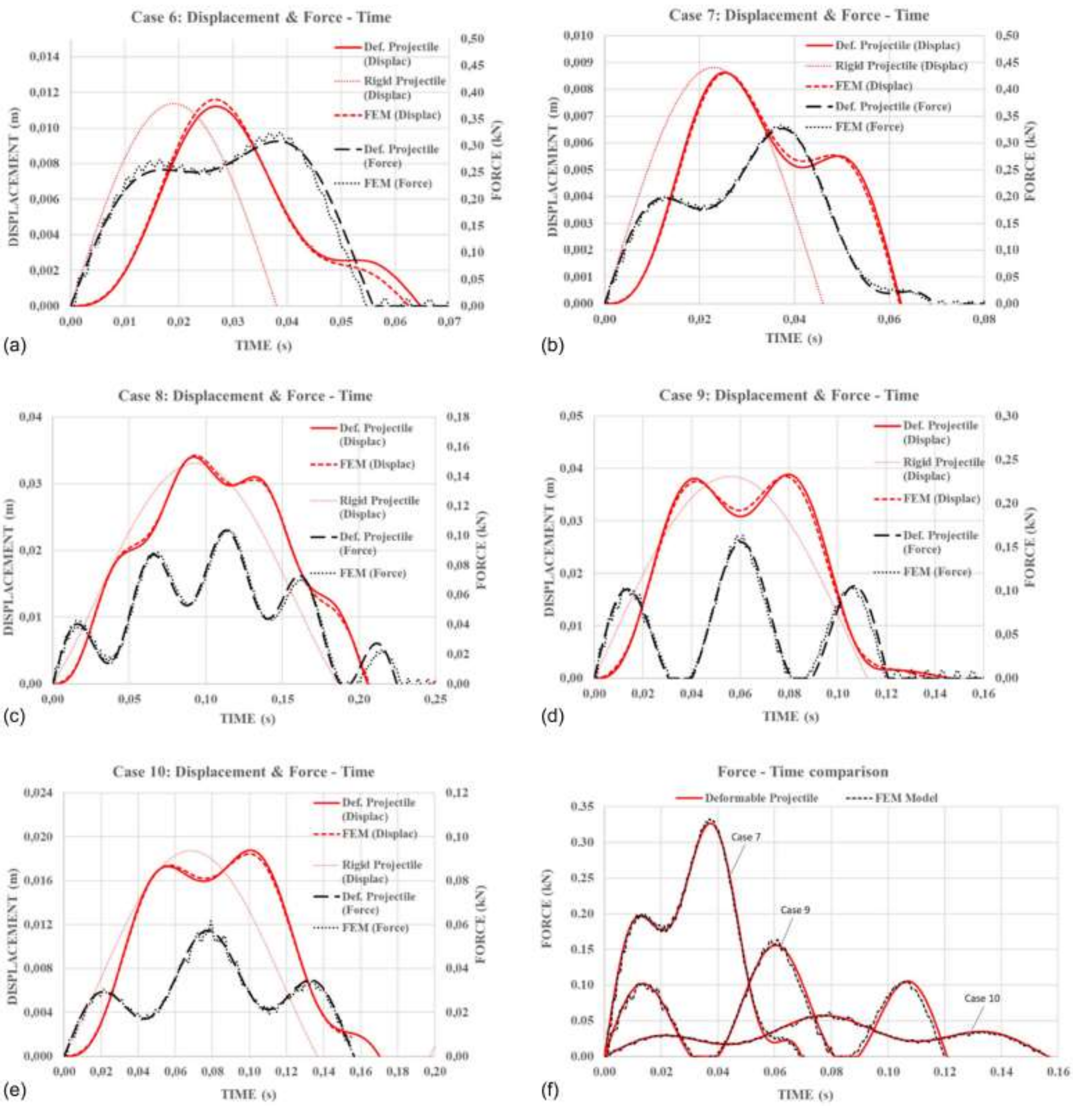

Fig. 8. Comparison between the results obtained using the simplified model considering *Deformable Projectile* and the FE models: (a) Case 6 (b) Case 7; (c) Case 8; (d) Case 9; (e) Case 10; and (f) Case 7, Case 9, and Case 10 comparison.

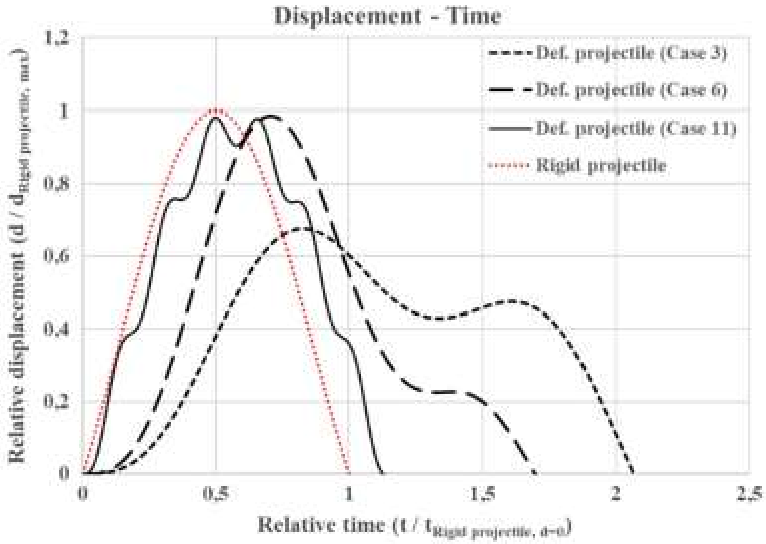

Fig. 9. Relative results of displacements for Case 3, Case 6, and Case 11.

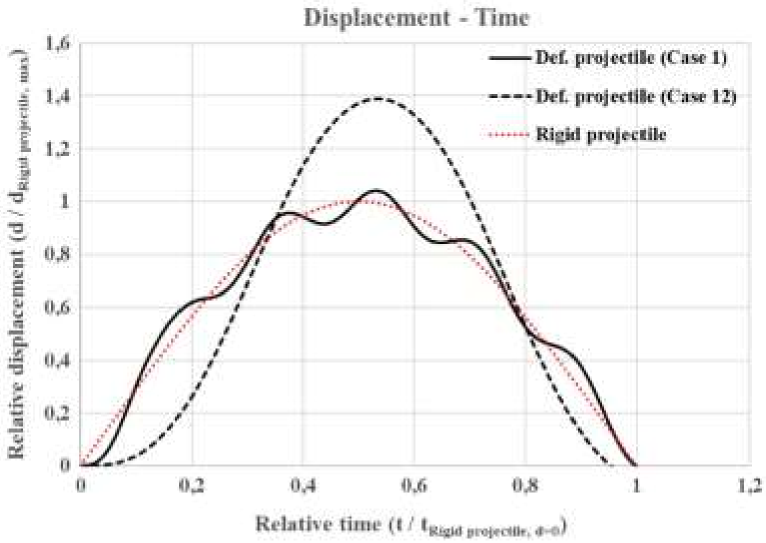

Fig. 10. Relative results of displacements for Case 1 and Case 12.

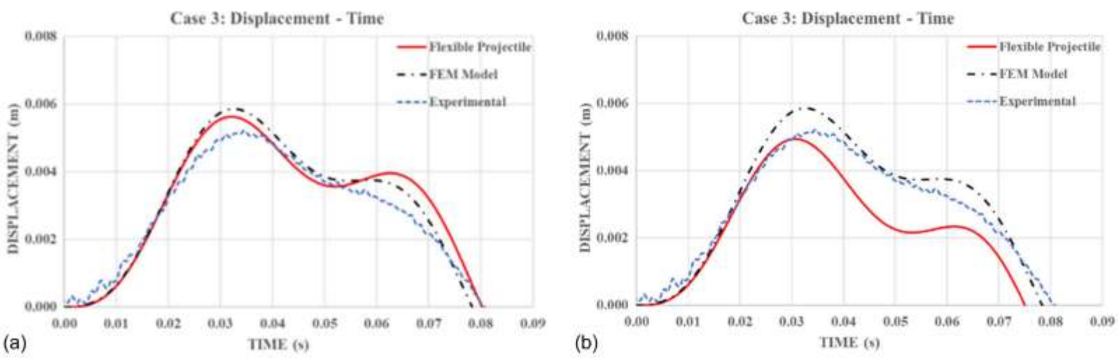

Fig. 11. Influence of gravity: (a) Case 3 results considering $g = 9.806\ \mathrm{m/s^2}$; and (b) Case 3 results considering $g = 0\ \mathrm{m/s^2}$.

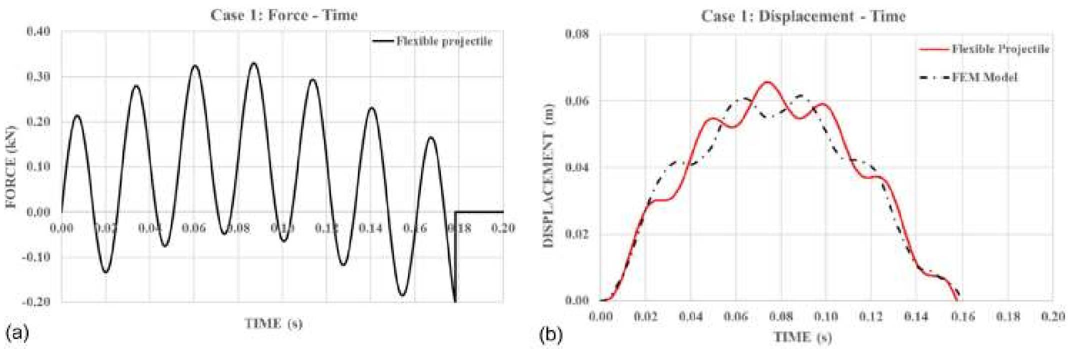

Fig. 12. Case 1 results if the contact force can cause tension forces: (a) contact force–time; and (b) displacement–time.

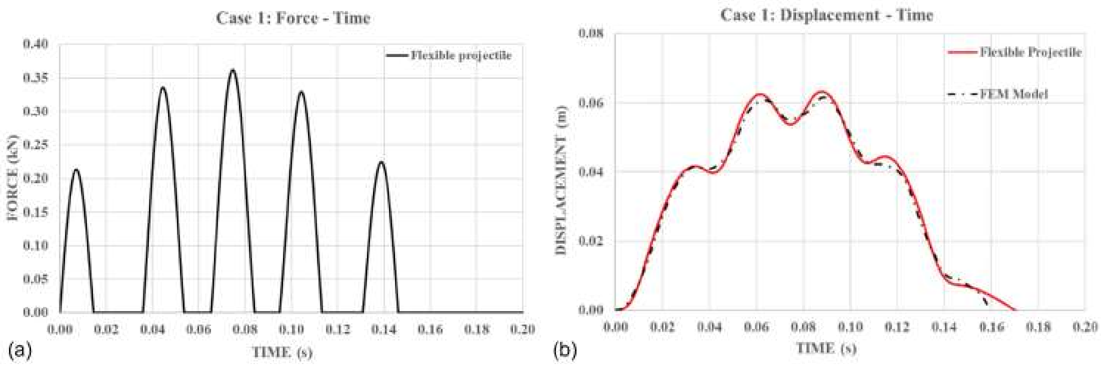

Fig. 13. Case 1 results if the contact force could cause tension forces: (a) contact force–time; and (b) displacement–time.